Defect-induced spin-glass magnetism in incommensurate spin-gap magnets

Eric C. Andrade[1] and Matthias Vojta[1]

[1] *Institut für Theoretische Physik, Technische Universität Dresden, 01062 Dresden, Germany*

PACS 75.10.Nr, 75.10.Jm, 75.50.Ee, 74.72.-h –

Abstract – We study magnetic order induced by non-magnetic impurities in quantum paramagnets with incommensurate host spin correlations. In contrast to the well-studied commensurate case where the defect-induced magnetism is spatially disordered but non-frustrated, the present problem combines strong disorder with frustration and, consequently, leads to spin-glass order. We discuss the crossover from strong randomness in the dilute limit to more conventional glass behavior at larger doping, and numerically characterize the robust short-range order inherent to the spin-glass phase. We relate our findings to magnetic order in both $BiCu_2PO_6$ and $YBa_2Cu_3O_{6.6}$ induced by Zn substitution.

Introduction. – Magnetic order induced by non-magnetic impurities is a remarkable phenomenon which has been observed in a wide variety of paramagnetic Mott insulators. It can be rationalized assuming dimer pairing of spins 1/2 in the host magnet: each non-magnetic impurity introduces one unpaired spin by breaking up a dimer. These impurity moments mutually interact by the exchange of gapped bulk excitations, with the interaction falling off exponentially as function of distance. If the host system features a bipartite lattice with antiferromagnetic spin correlations, the interactions between the impurity moments are non-frustrated, and consequently the ground state can be expected to be a long-range ordered antiferromagnet. This has been verified both numerically [1–3] and experimentally, with Zn-doped $CuGeO_3$ [4,5] and Mg-doped $TlCuCl_3$ [6] being prime examples.

Much less is known about impurity-induced magnetism in hosts with *incommensurate* (IC) correlations, realized e.g. in the Zn-doped spin ladder $BiCu_2PO_6$ [7–9] and also in the Zn-doped superconductor $YBa_2Cu_3O_{6.6}$, where recent experiments [10] have demonstrated the appearance of static order at an IC wavevector close to that of the host correlations. Based on the available experimental data, it has been suggested that the physics is not very different from the commensurate case.

In this paper, we instead argue that, although the mechanism of moment formation by impurities is similar in the commensurate and IC cases, the low-energy physics of these moments is vastly different. The IC case leads to frustration of the inter-moment interaction and thus to spin-glass behavior. The actual ordering temperature where spins freeze into a glassy state is suppressed as compared to the commensurate case due to frustration, leading to a broad temperature regime of slow fluctuations. The glassy regime is characterized by pronounced short-range order at (or near) the wavevector imprinted by the host correlations, with a correlation length which vanishes as the impurity concentration x is tuned towards zero. Dimensionality plays an important role: Glassiness is most pronounced if the host correlations are IC in three spatial directions, whereas a host with only one-dimensional (1d) incommensurability leads to a weakly glassy state with large magnetic correlation length.

In the body of this paper, we present general arguments and extensive numerical simulation data, comparing the commensurate and IC cases, which lead to the above conclusions. Our analysis sheds light onto a class of states which we believe is quite common to moderately disordered magnets, namely states with robust static short-range order combined with some amount of glassiness. We connect our results to the concrete experiments on doped spin-gap magnets in Refs. [7, 10].

Effective model. – We shall assume that a mechanism of dimer breaking underlies the formation of magnetic moments upon doping non-magnetic impurities. In its most general form, this mechanism relies on confinement of spinons in the host paramagnet and as such should apply to all spin-gap magnets with conventional spin-1 (triplon) excitations [11].

In the dilute limit of small x, there is a separation of energy scales, such that the impurity-induced moments provide the only degrees of freedom below the spin-gap energy Δ. Hence, the low-energy physics can be captured by an effective spin-S Heisenberg model involving the impurity moments $\vec{S}_i$ at random positions r_i only,

$$\mathcal{H}_{\rm eff} = -\sum_{ij} J_{ij} \vec{S}_i \cdot \vec{S}_j, \tag{1}$$

where S usually equals the bulk spin size. The interaction J_{ij} is dictated by the bulk magnetic properties. In a static linear-response approximation $J_{ij} = J_0^2 \chi(\vec{r}_{ij})$ where J_0 is of order of the bulk exchange coupling, and $\chi(\vec{r})$ is Fourier transform of the static bulk susceptibility $\chi(\vec{q})$. Hence, $|J_{ij}| \propto \exp(-r_{ij}/\xi_{\rm b})$ at long distances, where $\xi_{\rm b} \propto c/\Delta$ is the bulk correlation length and c a mode velocity [12–15]. The separation of energy scales requires $|J_{ij}| \ll \Delta$ which implies $\ell > \xi_{\rm b}$ where the average impurity distance $\ell = x^{-1/d}$ with $d = 3$. In this limit, the distribution of energy scales in the model (1) becomes broad: the maximum coupling for each spin, $J_i^{\rm max} = \max_j |J_{ij}|$, displays a strongly non-Gaussian distribution with large weight at small energies $J_i^{\rm max} \ll J_0$ [16].

Low-temperature order. – If the underlying lattice is bipartite and $\chi(\vec{q})$ is peaked at the antiferromagnetic wavevector $Q = (\pi, \pi, \ldots)$, then $\chi(\vec{r})$ changes sign from site to site. All interactions can be satisfied classically by antiferromagnetic order of the $\vec{S}_i$, which has been shown to survive even in for $S = 1/2$ [2,3,7,17,18].

In contrast, if $\chi(\vec{q})$ is peaked at an IC wavevector, the sign changes of $\chi(\vec{r})$ are irregular, and the model (1) is generically frustrated [19]. Thus, spin-glass behavior is expected, which we will characterize below.

It is worth noting that Eq. (1) is different from the Edwards-Anderson (E-A) spin-glass model [20]: The latter describes spins on a regular lattice with random couplings, whereas Eq. (1) features spins at random positions with deterministic couplings [21]. As a result, the J_{ij} in (1) display *correlated* disorder, in contrast to uncorrelated disorder usually assumed in the E-A model. Also, the broad distribution of couplings present in Eq. (1) is not a property of the standard E-A model.

Monte-Carlo simulations. – Being interested in qualitative properties at low temperatures T including the ordered phase, we consider three-dimensional (3d) systems (with possibly anisotropic couplings) in the classical limit first, and turn to quantum effects later. We randomly distribute $N_{\rm imp}$ unit vectors $\vec{S}_i$ on a cubic lattice of linear size L with periodic boundary conditions, yielding an impurity concentration $x = N_{\rm imp}/L^3$. The effective interaction J_{ij} is generated from Fourier transforming $\chi(\vec{q})$ which is approximated by the inverse of the gapped bulk triplon dispersion $\varepsilon(\vec{q})$ [12]:

$$J_{ij} = J_0^2 \frac{1}{L^3} \sum_{\vec{q}} \frac{e^{i\vec{q}\cdot\vec{r}_{ij}}}{\varepsilon(\vec{q})}. \tag{2}$$

We perform classical Monte-Carlo (MC) simulations of the effective model (1), with single-site updates using a combination of the heat-bath and microcanonical (or overrelaxation) methods [22]. We consider typically 10^5 MC steps per spin for the measurements, after discarding 10^5 MC steps for equilibration. For IC bulk correlations, we expect a (hardly-relaxing) spin-glass behavior, and to efficiently sample all spin configurations we employ the parallel-tempering algorithm [23]. Disorder averages are taken over $N_{\rm rl}$ impurity configurations, with $N_{\rm rl} = 400$ for $L = 16$ to $N_{\rm rl} = 50$ for $L = 40$.

From the MC data, we calculate thermodynamic observables, e.g., the specific heat C, as well as the neutron-scattering static structure factor

$$S(\vec{q}) = \frac{1}{N_{\rm imp}} \Big[\sum_{i,j} \Big\langle \vec{S}_i \cdot \vec{S}_j \Big\rangle e^{-i\vec{q}\cdot\vec{r}_{ij}} \Big]_{av}, \tag{3}$$

where $\langle \cdots \rangle$ denotes MC average and $[\cdots]_{av}$ average over disorder, and the sum runs over the $N_{\rm imp}$ impurity sites. In a long-range ordered phase $S(\vec{q})/N_{\rm imp} \to M^2 \delta_{\vec{q},\vec{Q}}$, where δ is the Kronecker delta and $\vec{Q}$ is the ordering wavevector. Note that $M \to 1$ as $T \to 0$, because the classical ground state is fluctuationless. The behavior of $S(\vec{q})$ near $\vec{Q}$ allows to extract the correlation length ξ_Q characterizing the *static* impurity order (ξ_Q is distinct from $\xi_{\rm b}$ [24]). To study signatures of spin-glass freezing, we also consider the spin-glass order parameter

$$q^{\alpha,\beta}(\vec{q}) = \frac{1}{N_{\rm imp}} \sum_i S_i^{\alpha(1)} S_i^{\beta(2)} e^{i\vec{q}\cdot\vec{r}_i}, \tag{4}$$

where α and β are spin components, and $^{(1)}$ and $^{(2)}$ denote two identical copies of the system ("replicas") containing the same impurity configuration. The spin-glass susceptibility is then defined as

$$\chi_{\rm SG}(\vec{q}) = N_{\rm imp} \sum_{\alpha,\beta} \Big[\Big\langle \big| q^{\alpha,\beta}(\vec{q}) \big|^2 \Big\rangle \Big]_{av}. \tag{5}$$

From $\chi_{\rm SG}(\vec{q})$ near $\vec{q} = 0$ we extract a spin-glass correlation length $\xi_{\rm SG}$. As $q^{\alpha,\beta}$ acquires long-range order in a spin-glass state, a divergence of $\xi_{\rm SG}$ signals the onset of spin-glass order, i.e., freezing.

In our finite-size simulations, the ordering (or freezing) temperature $T_{\rm g}$ is most efficiently extracted from the crossing points of $\xi(T)/L$ data for different L (with $\xi \equiv \xi_Q$ or $\xi \equiv \xi_{\rm SG}$), according to the scaling law $\xi/L = f(L^{1/\nu}(T - T_{\rm g}))$, where $f(x)$ is a scaling function and ν is the correlation length exponent [25].

Spin-glass order with short-range correlations. – A detailed comparison between the cases of commensurate and IC host correlations is in Fig. 1. We have used the bulk triplon dispersions $\varepsilon(\vec{q})$ in Figs. 1a and b, respectively, to generate the J_{ij} according to Eq. (2). Fig. 1a has a single minimum at (π, π, π) whereas Fig. 1b has eight minima at $(\pi \pm \delta, \pi \pm \delta, \pi \pm \delta)$ with $\delta = \pi/4$

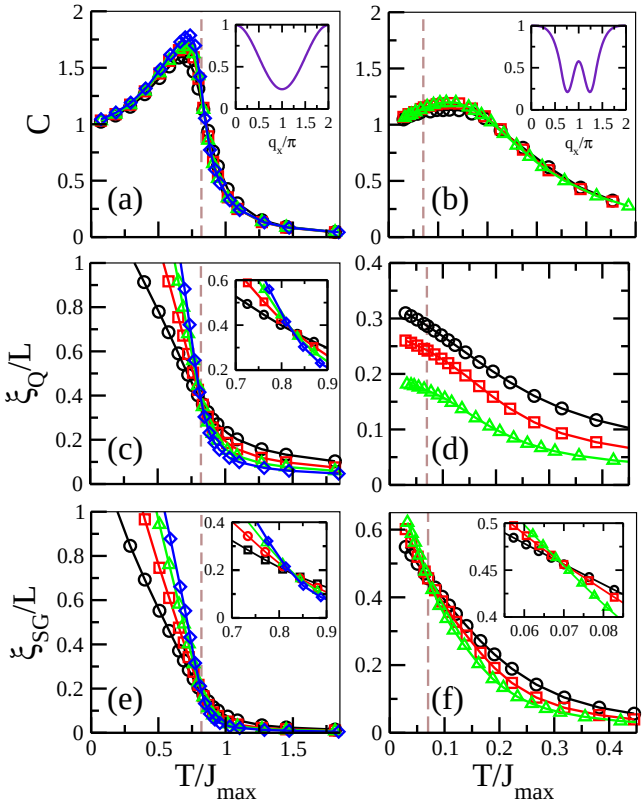

Figure 1: Classical MC results for the ordering process of impurity moments described by $\mathcal{H}_{\rm eff}$ (1), in the cases of commensurate (left) and incommensurate (right) bulk correlations, for $x = 2\%$ and different system sizes: $L = 16$ (○), 24 (□), 32 (△), and 40 (◇). (a, b) Specific heat C as a function of T. Insets: Host dispersion $\varepsilon(\vec{q})$, normalized by its bandwidth, along $\vec{q} = (q_x, \pi, \pi)$ and $\vec{q} = (q_x, \frac{3}{4}\pi, \frac{3}{4}\pi)$, respectively. (c, d) Magnetic correlation length ξ_Q divided by L as function of T for $\vec{Q} = (\pi, \pi, \pi)$ and $(\frac{3}{4}\pi, \frac{3}{4}\pi, \frac{3}{4}\pi)$, respectively. (e, f) T dependence of the spin-glass correlation length $\xi_{\rm SG}/L$. The crossing point for different L defines the ordering/freezing temperature $T_{\rm g}$ (vertical dashed lines). Insets in c, e, f show a zoom on ξ/L near $T_{\rm g}$. Error bars are smaller than the symbol size.

[19]. In both cases we have used $x = 2\%$ and chosen $\varepsilon(\vec{q})$ such that $\xi_{\rm b} \simeq 3a$. Energies are given in units of $J_{\rm max} = |J_{ij}(r_{ij} = 1)|$ [26].

All features in Figs. 1a,c,e consistently point towards the onset of long-range magnetic order at $T_{\rm N} \approx 0.82 J_{\rm max}$: a unique crossing point in both ξ_Q/L and $\xi_{\rm SG}/L$ at the same $T_{\rm N}$ [27] and a specific-heat maximum which both sharpens and moves towards $T_{\rm N}$ upon increasing L.

The results for the IC case, Figs. 1b,d,f, are strikingly different. A crossing is present only in $\xi_{\rm SG}/L$, indicating a transition into a spin-glass state at a low $T_{\rm g} \approx 0.07 J_{\rm max}$ [21], while no crossing is observed in ξ_Q/L. The peak in $C(T)$ is broad and occurs at a temperature considerably larger than the freezing temperature (here $T_{peak} \approx 2T_{\rm g}$). The origin is the emergence of short-range magnetic order far above $T_{\rm g}$ [20], which is nicely visible in the gradual increase of ξ_Q, Fig. 1d. The momentum dependence of

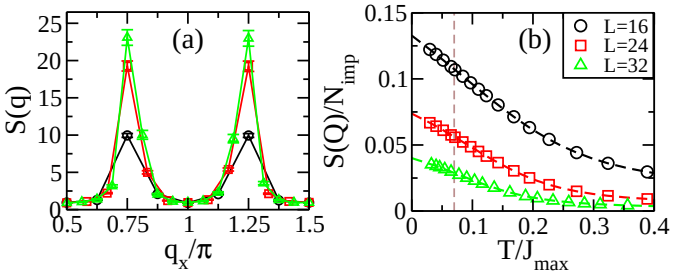

Figure 2: Structure factor $S(\vec{q})$ for IC bulk correlations and the same parameters as in Fig. 1. a) Momentum dependence along $\vec{q} = (q_x, \frac{3}{4}\pi, \frac{3}{4}\pi)$ at $T = T_g/2$. b) $S(\vec{Q})$ at $\vec{Q} = (\frac{3}{4}\pi, \frac{3}{4}\pi, \frac{3}{4}\pi)$ divided by $N_{\rm imp}$ as function of T.

the structure factor $S(\vec{q})$, Fig. 2a, indeed shows peaks at the wavevectors $\vec{Q}$ corresponding to the minima of $\varepsilon(\vec{q})$. However, those peaks grow slower than the system size, Fig. 2b, indicating static short-range order with a vanishing magnetic order parameter M [28].

The fact that $S(\vec{q})$ peaks at (or near) $\vec{Q}$ in the IC case is non-trivial given that the system is both strongly disordered and frustrated. It may be rationalized by considering the dense limit $x \to 1$: Here, the classical $\mathcal{H}_{\rm eff}$ (1) is minimized by a spiral state with ordering wavevector $\vec{Q}$ for which the Fourier transform of J_{ij} has a maximum [29]. Our results show that, upon dilution, this spiral order then becomes both short-ranged and glassy.

Doping dependence. – The model (1) has two characteristic length scales as input, namely ℓ and $\xi_{\rm b}$, and one expects that their ratio $\ell/\xi_{\rm b}$ is dominant in determining the physical behavior. Clearly, $\ell \gg \xi_{\rm b}$ represents a strongly disordered regime, with a broad distribution of coupling constants and suppressed ordering temperature, whereas $\ell \ll \xi_{\rm b}$ can be expected to lead to a more conventional state (still being glassy in the IC case). Many experiments are in an intermediate regime of $\ell \gtrsim \xi_{\rm b}$ [7].

We have calculated the ordering/freezing temperature $T_{\rm g}$ as function of doping x at fixed $\xi_{\rm b}$, with results shown

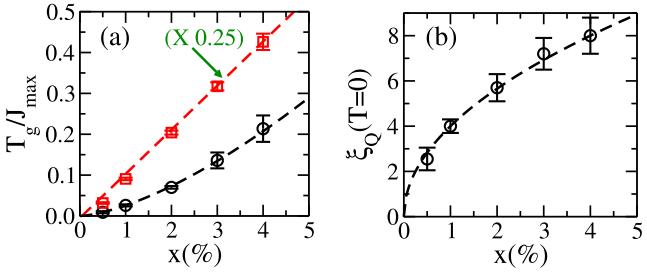

Figure 3: a) Ordering temperature (rescaled by 0.25, □) for commensurate and freezing temperature (○) for IC host correlations, as function of the impurity concentration x. b) Magnetic correlation length ξ_Q for IC host correlations, extrapolated to $T = 0$ and $L = \infty$, as function of x. (Dashed lines are guides to the eye, see text.)

in Fig. 3a. As expected, T_g/J_{max} is significantly smaller in the IC case as compared to the commensurate one due to frustration. $T_g(x)$ is approximately linear in this range of x for the commensurate case, while it shows sublinear behavior for the IC case, which is well fitted by $T_g \propto x^{1.6}$ (dashed). For smaller ξ_b also the commensurate case shows sublinear behavior (not shown). Experimentally, a linear $T_g(x)$ is frequently observed [7], while for very small x sublinear behavior has been found [5], consistent with our numerical results and previous ones for the commensurate case [7,30].

Thus, $T_g(x)$ appears to be generically sublinear at small x before it crosses over to approximately linear behavior. It has been suggested that the typical value of the couplings J_{ij} governs T_g in the dilute limit $x \to 0$, while the average coupling is relevant in the more dense case where $T_g(x)$ is found to be linear [7,31]. We note, however, that at present there is no analytical understanding of the behavior of $T_g(x)$ in the dilute limit.

Fig. 3b shows the magnetic correlation length ξ_Q in the IC case, extrapolated to $T = 0$ and $L = \infty$. Remarkably, $\xi_Q(x)$ appears to vanish as $x \to 0$, i.e., the spatial correlations between the impurity moments diminish in the dilute limit. Qualitatively, such a $\xi_Q \ll \ell$ corresponds weakly correlated isolated impurities, whereas $\xi_Q \gtrsim \ell$ can be associated with a spin glass formed from clusters of correlated impurities with cluster size ξ_Q. (For the parameters in Fig. 3b, $\xi_Q \approx \ell$ at $x \approx 1\%$.)

Dimensionality. – We have also considered spatially anisotropic cases where the IC host correlations only extend along one or two directions (dubbed 1dIC and 2dIC), whereas the correlations are commensurate (and weaker) in the remaining direction(s) – this situation applies to various quasi-1d or quasi-2d materials.

The sample results in Fig. 4 demonstrate a clear trend with dimensionality of the IC correlations: The 1dIC case in Fig. 4 (left) displays frustration in only one direction, therefore magnetic correlations are longer-ranged and consequently glassiness is weak. As can be seen from Fig. 4a, ξ_Q exceeds our largest system size at low T. However, from both the shift of the crossing points with system size (Fig. 4a), i.e., the absence of a unique crossing point, and the fact that $S(\vec{Q})/N_{imp}$ extrapolates to zero as $L \to \infty$ we can safely conclude that there is no conventional magnetic order, but only spin-glass order at low T. Turning to the 2dIC case in Fig. 4 (right), we observe that this qualitatively resembles the situation in 3d, where ξ_Q remains small below T_g.

We have studied the systematics of $T_g(x)$ in the spatially anisotropic cases, and find the general trend – sublinear behavior at small x and linear behavior at larger x – to be obeyed here as well. Interestingly, $T_g(x)/J_{max}$ is only suppressed by factors 1.3—4 by 1dIC correlations as compared to the fully commensurate case (for correlation lengths as in Fig. 4a and $0.5\% \le x \le 2\%$); this can be contrasted to the suppression by a factor of 10 or more found for the 3d incommensurate situation, Fig. 3a.

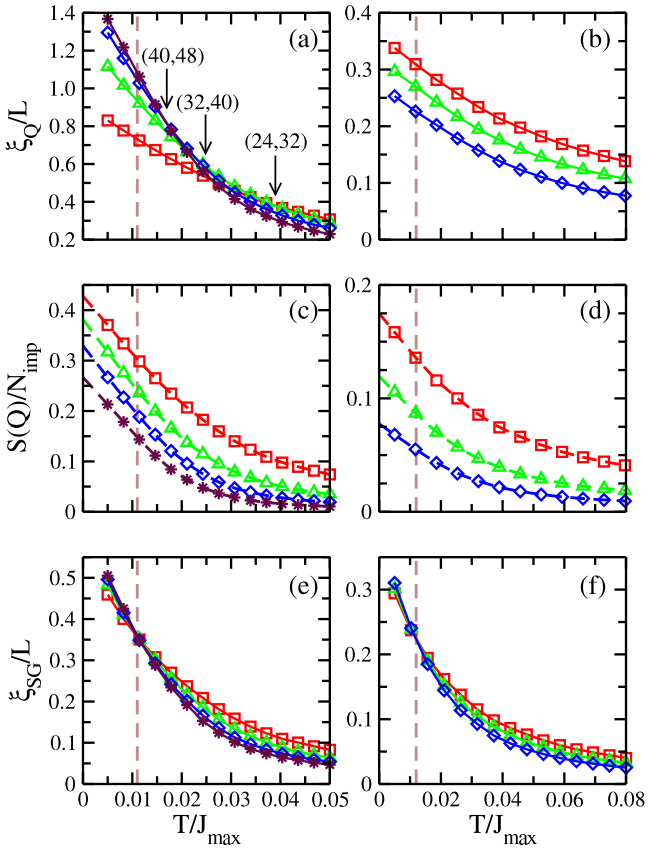

Figure 4: Ordering process of impurity moments, now for spatially anisotropic incommensurability, comparing 1dIC with $\vec{Q} = \left(\frac{3}{4}\pi, \pi, \pi\right)$ (left) and 2dIC with $\vec{Q} = \left(\frac{3}{4}\pi, \frac{3}{4}\pi, \pi\right)$ (right). The bulk correlation lengths are $\xi_b/a \approx (4, 1.5, 1.5)$ (left) and $\xi_b/a \approx (3.3, 3.3, 1.3)$ (right) in the three directions. (a,b) Magnetic correlation length $\xi_Q(T)/L$ along an incommensurate direction for $x = 0.5\%$ and system sizes $L = 24\,(\square)$, $32\,(\triangle)$, $40\,(\lozenge)$, and $48\,(*)$. In (a), the arrows indicate the crossing points of the curves for different pairs of L. (c,d) Structure factor $S(\vec{Q})/N_{imp}$. (e,f) Spin-glass correlation length $\xi_{SG}(T)/L$. For both 1dIC and 2dIC, a clear crossing point in ξ_{SG}/L is observed which allows to extract the T_g (vertical dashed). For a discussion see text.

Quantum effects and real-space renormalization group. – Our MC simulations presented so far neglect quantum fluctuations of the impurity moments. (Quantum effects in the *bulk* are crucial for the moment formation; those are taken into account in writing down Eq. (1).) A central question is whether the classical order of the $\vec{S}_i$ survives for $S = 1/2$. For the commensurate case, both real-space renormalization group (RSRG) studies of Eq. (1) [17,18] and numerical simulations of vacancy-doped quantum paramagnets [2,3,7] show that the answer is yes. In particular, the RSRG shows the generation of large spins in the course of the RG, which indicates magnetic order at low T (instead of a random-singlet ground state) – the same has been found for random Heisenberg

models [32].

We have implemented the RSRG for the model in Eq. (1) with quantum spins 1/2 following Refs. [17,18,32]. In this procedure, we consider all possible pairs of spins in the system and calculate the energy gap between their ground state and the first excited multiplet. We then select the pair $(\vec{S}_1, \vec{S}_2)$ with the largest energy gap Δ_{12} (which may then be identified with the system temperature). One RG step is characterized by the decimation of the pair $(\vec{S}_1, \vec{S}_2)$ according to the rules in Refs. [17,18,32], where the pair is either replaced by a single effective spin (representing a spin cluster) or removed completely (if the ground state of the pair was a singlet). We iterate the decimation procedure up to the last effective spin, or until we decimate the last spin singlet.

Selected RSRG results for the model (1), Fig. 5, demonstrate the formation of large spins upon decimation for *both* commensurate and IC bulk correlations, very similar to the results in Refs. [17, 18, 32]. Both the average spin size $S_{\rm eff}$ and the average number of original spins $N_{\rm eff}$ of the remaining spin clusters diverge in the course of the RG, indicating magnetic order. This divergence can be described as $S_{\rm eff} \propto N_{\rm eff}^{\zeta}$ [32], and we estimate ζ as 0.51 for commensurate and 0.58 for IC bulk correlations, respectively. Importantly, the formation of a random-singlet state would instead imply that both $S_{\rm eff}$ and $N_{\rm eff}$ remain small. The main difference between the commensurate and IC cases in Fig. 5 is that the high-temperature region where such random-singlet formation dominates is much extended for IC correlations, reflecting a broad regime of slow fluctuations above $T_{\rm g}$, as anticipated above. Finally, we note that the RSRG procedure is not able to distinguish between conventional long-range magnetic order and spin-glass order, because the effect of frustration – which requires at least three spins – cannot be fully captured within the pairwise decimation procedure.

We conclude that the RSRG confirms the tendency of Eq. (1) toward low-temperature order: Quantum effects do not qualitatively change the predictions of the classical MC simulations, although they are important in a regime above $T_{\rm g}$ where the formation of random singlets dominates in the dilute limit $\ell \gg \xi_{\rm b}$. Hence, the classical MC simulations cannot be expected to describe the thermodynamics at and above $T_{\rm g}$, but they capture the physics of the low-T ordered state, with our $T_{\rm g}$ being an upper bound to the true freezing temperature.

Experiments. – $BiCu_2PO_6$ is a spin-ladder material with 1dIC correlations [8]. Hence, we expect weakly glassy behavior upon Zn doping [7, 9]. Indeed, deviations between experimental data and the results of numerical simulations (which do not account for frustration) have been observed [9] and tentatively assigned to the effect of magnetic frustration. The fact that the experimental $T_{\rm g}$ of $BiCu_2PO_6$ is not very different from that of doped commensurate spin-gap magnets with similar energy scales and correlation lengths [7] is consistent with our finding

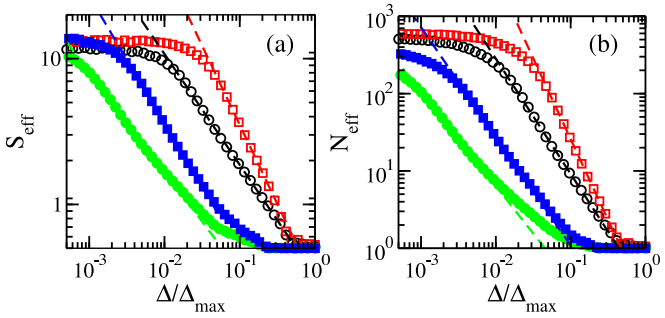

Figure 5: RSRG results for the model (1) with quantum spins 1/2, both for $x = 1\%$, $L = 50$ (○,●) and $x = 2\%$, $L = 40$ (□,■), with $N_{\rm rl} = 10^4$. Open (full) symbols correspond to commensurate (IC) bulk correlations, with parameters as in Fig. 1. (a) Size of the effective cluster spin moment $S_{\rm eff}$, averaged over the remaining (active) cluster spins, as a function of the energy scale Δ (equivalent to temperature), normalized by its maximal value. (b) Number of original spins-1/2 per cluster, averaged over the remaining (active) cluster spins, as a function of $\Delta/\Delta_{\rm max}$. The dashed lines are power-law fits, and the plateaus at small Δ arise from the finite value of $N_{\rm imp}$.

that 1dIC correlations only cause a moderate suppression of $T_{\rm g}$. From our results we predict a strongly sublinear x dependence of $T_{\rm g}$ for $x < 1\%$.

The superconductor $YBa_2Cu_3O_{6.6}$ displays a sizeable spin gap, with 2% of Zn substitution inducing static short-range magnetic order peaked at a 2dIC wavevector close to that of the host correlations [10]. For cuprates, experiments indicate that both IC magnetic correlations and IC magnetic order (the latter occurs at lower oxygen doping in Zn-free $YBa_2Cu_3O_{6+\delta}$ as well as in other cuprates) can be described as collective magnetism (as opposed to simple Fermi-surface nesting) originating from the tendency towards stripe formation [33]. Therefore it is reasonable to assume that the physics of impurity moments in spin-gapped cuprates can be captured by $\mathcal{H}_{\rm eff}$ (1) [11], and consequently we predict the magnetically ordered state in Zn-substituted $YBa_2Cu_3O_{6.6}$ to be glassy. (In fact, Ni substitution in $La_{1.85}Sr_{0.15}CuO_4$ has been shown to induce spin-glass order even in the superconducting state [34].) Based on Fig. 3b we also predict the width of the magnetic Bragg peaks to increase for smaller x which can be checked by future neutron scattering experiments.

Conclusions. – We have investigated the magnetism of impurity moments in incommensurate spin-gap magnets, which we have shown to be frustrated, leading to static order at low T akin to that of a cluster spin glass – in strong contrast to the commensurate case where the low-T state is a disordered, but unfrustrated antiferromagnet.

Our results call for further experiments on impurity-doped magnets, in particular a characterization of spin-glass behavior of the low-T order, e.g., by ac susceptibility measurements. Theoretically, it will be interesting

to study the interplay of spin-glass and quantum effects beyond the real-space RG procedure. Particularly fascinating will be the connection of the zero-field spin glass to the Bose-glass phase expected in an applied field [35].

We thank P. Henelius, B. Keimer, C. Rüegg, and C. Timm for illuminating discussions. This research was supported by the DFG through FOR 960 and GRK 1621.

References

[1] M. Imada and Y. Iino, J. Phys. Soc. Jpn. **66**, 568 (1997).
[2] C. Yasuda *et al.*, Phys. Rev. B **64**, 092405 (2001).
[3] S. Wessel *et al.*, Phys. Rev. Lett. **86**, 1086 (2001).
[4] M. Hase *et al.*, Phys. Rev. Lett. **71**, 4059 (1993).
[5] K. Manabe *et al.*, Phys. Rev. B **58**, R575 (1998).
[6] A. Oosawa, T. Ono, and H. Tanaka, Phys. Rev. B **66**, 020405(R) (2002).
[7] J. Bobroff *et al.*, Phys. Rev. Lett. **103**, 047201 (2009) and references therein.
[8] A. A. Tsirlin *et al.*, Phys. Rev. B **82**, 144426 (2010).
[9] L. K. Alexander *et al.*, Phys. Rev. B **81**, 054438 (2010) .
[10] A. Suchanek *et al.*, Phys. Rev. Lett. **105**, 037207 (2010).
[11] M. Vojta, C. Buragohain, and S. Sachdev, Phys. Rev. B **61**, 15152 (2000).
[12] M. Sigrist and A. Furusaki, J. Phys. Soc. Jpn. **65**, 2385 (1996).
[13] Strictly, the linear-response assumption is not justified in deriving J_{ij}, as the impurity-induced moments couple to the bulk with J_0, i.e., a relative strength of order unity. While this is relevant for prefactors of J_{ij}, it will not change its qualitative dependence of r_{ij}.
[14] In magnets with strong frustration and weak dimerization, it is possible to reach a regime of *weak confinement* [15], with a bulk confinement length $\xi_{\rm b}^{\rm conf}$ being larger than the magnetic correlation length $\xi_{\rm b}$. Then, a nonmagnetic impurity will still induce a magnetic moment, but $\xi_{\rm b}^{\rm conf}$ (instead of $\xi_{\rm b}$) determines the size of the polarization cloud near the impurity, and the effective coupling in Eq. (1) becomes $|J_{ij}| \propto \exp(-r_{ij}/\xi_{\rm b}^{\rm conf})$.
[15] R. L. Doretto and M. Vojta, Phys. Rev. B **80**, 024411 (2009).
[16] In one dimension, one can show that the distribution of the $J_i^{\rm max}$ in model (1) displays a power-law divergence in the dilute limit, with an x-dependent exponent [12].
[17] R. Melin, Eur. Phys. J. B **16**, 261 (2000).
[18] N. Laflorencie, D. Poilblanc, and M. Sigrist, Phys. Rev. B **71**, 212403 (2005); N. Laflorencie and D. Poilblanc, J. Phys. Soc. Jpn. Suppl. **74**, 277 (2005).
[19] Frustration arises also for long-period commensurate $\vec{Q}$.
[20] K. H. Fischer and J. A. Hertz, *Spin Glasses* (Cambridge University Press, Cambridge, 1991).
[21] A study of the critical behavior near the putative spin-glass transition is beyond the scope of this work. We note that the correlated disorder present in model (1) might render it different from that of the E-A spin glass model.
[22] B. A. Berg, *Markov Chain Monte Carlo Simulations and Their Statistical Analysis* (World Scientific, Singapore, 2004).
[23] K. Hukushima and K. Nemoto, J. Phys. Soc. Jpn. **65**, 1604 (1996).
[24] ξ_Q reflects equal-time correlations of the static impurity moments, while $\xi_{\rm b}$ parametrizes the $\omega = 0$ bulk susceptibility. In particular, $\xi_Q < \xi_{\rm b}$ is possible and corresponds to frustration (i.e. destructive interference) between the polarization clouds around each impurity [7, 9, 11].
[25] L. W. Lee and A. P. Young, Phys. Rev. B **76**, 024405 (2007); D. X. Viet and H. Kawamura, *ibid.* **80**, 064418 (2009).
[26] $J_{\rm max}/J_0 \approx 0.28$ (commensurate) and $J_{\rm max}/J_0 \approx 0.15$ (IC).
[27] We expect the magnetic transition to be in the 3d Heisenberg universality class even in the presence of disorder, as the correlation length exponent $\nu \approx 0.71$ fulfills the Harris criterion $\nu > 2/d$. However, from the data in Fig. 1c we extract a different $\nu \approx 0.79$ which we attribute to large subleading corrections for our small systems.
[28] In the IC case, we did not detect any order in scalar or vectorial spin correlations.
[29] K. Yosida, *Theory of Magnetism* (Springer, Berlin, 1996).
[30] N. Laflorencie *et al.*, Phys. Rev. B. **69**, 212412 (2004).
[31] A theoretical discussion of a similar crossover, in the context of dilute graphene antiferromagnets, is presented in: T. Fabritius *et al.*, Phys. Rev. B **82**, 035402 (2010).
[32] Y.-C. Lin *et al.*, Phys. Rev. B **68**, 024424 (2003).
[33] M. Vojta, Adv. Phys. **58**, 699 (2009).
[34] A. Malinowski *et al.*, Phys. Rev. B **84**, 024409 (2011).
[35] R. Yu *et al.*, Phys. Rev. B **82**, 134437 (2010).